Self-assembled nanospheres with multiple endohedral binding sites pre-organize catalysts and substrates for highly efficient reactions

Wang, Q.; Gonell Gomez, S.; Leenders, S.H.A.M.; Dürr, M.; Ivanović-Burmazović, I.; Reek, J.N.H.

DOI
10.1038/NCHEM.2425

Publication date
2016

Document Version
Final published version

Published in
Nature Chemistry

License
Article 25fa Dutch Copyright Act

nature chemistry

ARTICLES

PUBLISHED ONLINE: 11 JANUARY 2016 | DOI: 10.1038/NCHEM.2425

Self-assembled nanospheres with multiple endohedral binding sites pre-organize catalysts and substrates for highly efficient reactions

Qi-Qiang Wang[1†], Sergio Gonell[1], Stefan H. A. M. Leenders[1], Maximilian Dürr[2], Ivana Ivanović-Burmazović[2] and Joost N. H. Reek[1*]

Tuning reagent and catalyst concentrations is crucial in the development of efficient catalytic transformations. In enzyme-catalysed reactions the substrate is bound—often by multiple non-covalent interactions—in a well-defined pocket close to the active site of the enzyme; this pre-organization facilitates highly efficient transformations. Here we report an artificial system that co-encapsulates multiple catalysts and substrates within the confined space defined by an $M_{12}L_{24}$ nanosphere that contains 24 endohedral guanidinium-binding sites. Cooperative binding means that sulfonate guests are bound much more strongly than carboxylates. This difference has been used to fix gold-based catalysts firmly, with the remaining binding sites left to pre-organize substrates. This strategy was applied to a Au(I)-catalysed cyclization of acetylenic acid to enol lactone in which the pre-organization resulted in much higher reaction rates. We also found that the encapsulated sulfonate-containing Au(I) catalysts did not convert neutral (acid) substrates, and so could have potential in the development of substrate-selective catalysis and base-triggered on/off switching of catalysis.

In the past decades tremendous progress in the area of supramolecular chemistry has stimulated the field of catalysis to implement supramolecular strategies and has led to the emergence of the field of supramolecular catalysis[1–3]. The use of non-covalent interactions to generate bidentate ligands from ligand building blocks is now well established[4,5], and more recently it has been demonstrated that interactions between the substrate and the functional groups of the catalyst can lead to enhanced catalytic activity and unprecedented selectivity by way of substrate pre-organization at the metal centre[6]. In parallel, catalysis in confined spaces has been developed; by placing catalysts in cages, a well-defined second coordination sphere around a catalyst is generated that facilitates new ways to control the properties of the catalysts. For this purpose, various cavity-containing supramolecular scaffolds, which include covalent macrocycle/cage compounds[7–9] and metal self-assembled or hydrogen-bonding assembled capsules[9–17], have been explored for a number of catalytic transformations. The introduction of catalysts (catalytic sites) in molecular cages usually proceeds either via covalent attachment of the catalyst or via direct encapsulation using, for example, hydrophobic effects[7–17]. The covalent attachment is generally associated with long synthetic protocols. Whereas direct encapsulation seems synthetically more convenient, it is rather challenging to find the appropriate capsule that both accommodates the catalyst precursor, and all its intermediate states, and allows co-encapsulation of the substrate. The best of both worlds may be a molecular capsule that is functionalized with binding motifs that can accommodate catalysts that have complementary binding units. This approach could be viable for both small capsules that bind one catalyst and larger spheres that can accommodate multiple catalysts. Along these lines, we herein report self-assembled $M_{12}L_{24}$ nanospheres[18–21] with multiple (24) endohedral guanidinium groups that function as hydrogen-bond motifs, that can strongly bind sulfonate groups and that weakly bind carboxylates. This difference in binding behaviour allows the selective encapsulation of sulfonate-containing gold catalysts and, at the same time, carboxylate-functionalized substrates are pre-organized in close proximity to these catalysts by weaker binding in the same sphere. This pre-organization effect leads to dramatically enhanced reaction rates in the cyclization reaction of acetylenic acid into enol lactone. As the neutral substrates (in the absence of a base) have no affinity for the sphere, it is a simple matter to switch the catalyst activity on/off by a base-induced gating mechanism.

Results and discussion

The group of Fujita has developed a very powerful strategy to generate $Pd_{12}L_{24}$ nanospheres based on the self-assembly of 12 Pd^{2+} ions and 24 bent bialkynylpyridine ligands[18–21]. The beauty of the system not only consists in the intriguing three-dimensional large hollow structure, but also in its facile endohedral or exohedral functionalization by just placing functional groups onto the organic building blocks. Recently, our group applied this strategy to functionalize the sphere endohedrally with up to 24 gold complexes ($[R_3PAuCl]$ (R = aryl)). The estimated local gold concentration was above 1 M, and this high local concentration resulted in the activation of otherwise inactive gold chloride complexes in the hydroalkoxylation of allenol and cycloisomerization of 1,6-enyne reactions[22]. To facilitate the non-covalent anchoring of the catalysts, we set out to functionalize the organic building blocks with guanidinium-binding motifs as they can form complexes via hydrogen bonding with carboxylates and sulfonates[23,24]. The high local concentration of guanidinium could lead to the formation of

[1]Homogeneous, Supramolecular and Bio-Inspired Catalysis, Van 't Hoff Institute for Molecular Sciences, University of Amsterdam, Science Park 904, Amsterdam 1098XH, The Netherlands. [2]Lehrstuhl für Bioanorganische Chemie, Department Chemie und Pharmazie, Friedrich-Alexander-Universitaet Erlangen, Egerlandstrasse 3, Erlangen 91058, Germany. †Present address: CAS Key Laboratory of Molecular Recognition and Function, Institute of Chemistry, Chinese Academy of Sciences (ICCAS), Beijing 100190, China. *e-mail: j.n.h.reek@uva.nl

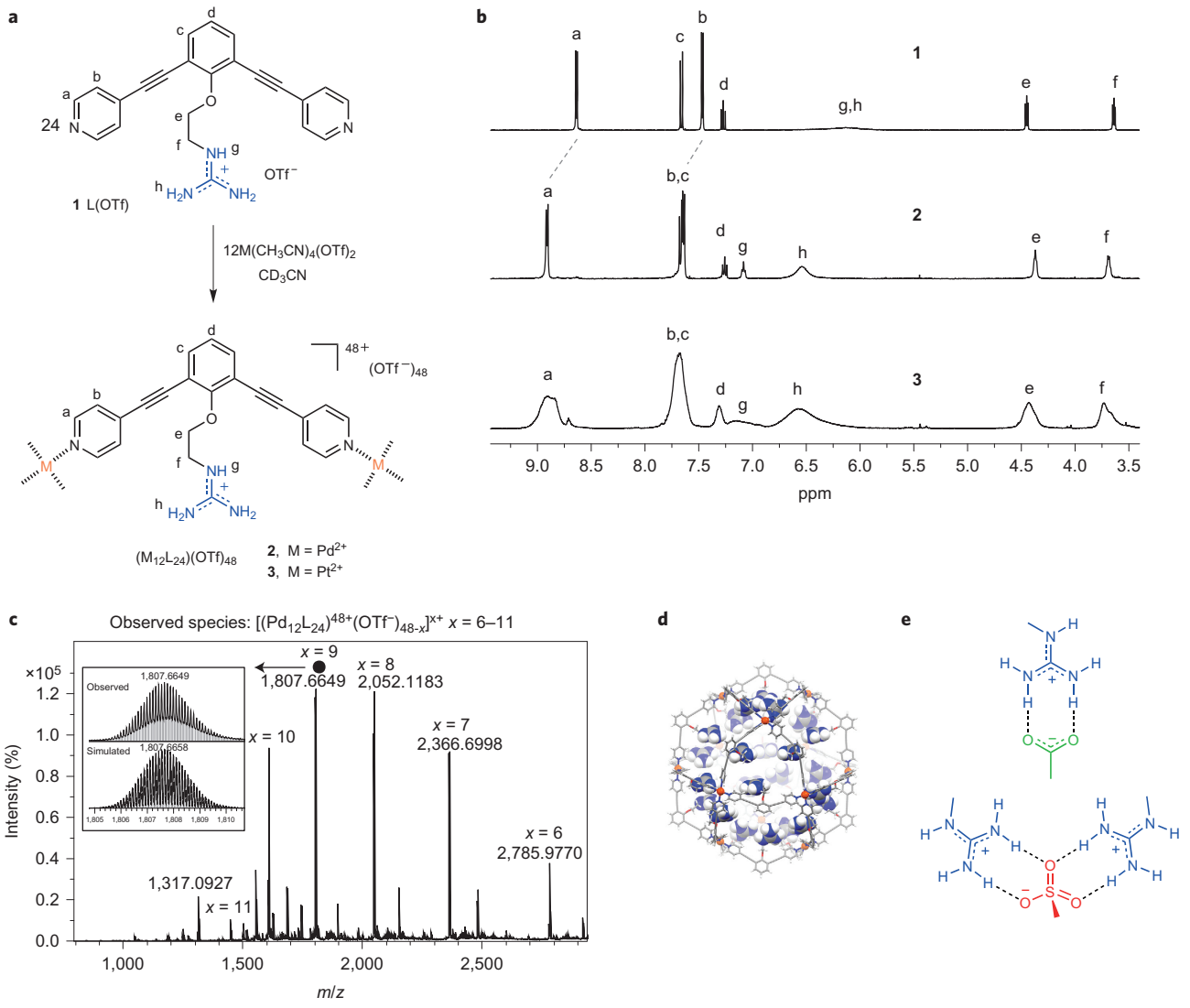

Figure 1 | Synthesis and characterization of the $M_{12}L_{24}$ spheres that bear endohedral guanidinium-binding sites. a, Molecular structure of building block **1** and the assembly of spheres **2** and **3**. **b**, ^{1}H NMR spectra (298 K, CD_3CN) of building block **1** and spheres **2** and **3**. **c**, CSI-MS of sphere **2** with assignment of the observed species. **d**, PM3-Spartan-modelled $Pd_{12}L_{24}$ sphere with the guanidinium groups shown in space-filling mode. **e**, Plausible binding mode for the guanidinium to carboxylate (top) and the cooperative binding mode of two guanidinium sites to one sulfonate guest (bottom).

hydrogen-bonded networks with a sulfonated guest and, as such, could also lead to an increased binding affinity[25–27].

The guanidinium-containing building block **L**(OTf) (**1**) (OTf, OSO_2CF_3) was readily synthesized from 2,6-dibromophenol through five synthetic steps with a moderate-to-excellent yield for each step (for the synthesis and a full characterization, see the Supplementary Information). The crystal structure of **1** showed that the guanidinium group forms two hydrogen bonds with the weakly coordinated counterion OTf^- ($N–H^h\cdots O = 2.851$, 3.020 Å (see Supplementary Fig. 12)). When building block **1** (2 equiv.) was stirred in CD_3CN at 50 °C in the presence of 1 equiv. $Pd(CH_3CN)_4(OTf)_2$, the desired single $Pd_{12}L_{24}$ species (**2**) was formed overnight as indicated by the one clear set of proton signals in the ^{1}H NMR spectra with the characteristic downfield shifts for the pyridine protons (H^a and H^b) (Fig. 1b). The guanidinium proton signals (H^g and H^h) also shifted downfield, which may indicate the formation of hydrogen bonds as a consequence of the high local concentration. Importantly, the diffusion-ordered spectroscopy (DOSY) NMR spectra show a clear single band at log $D = -9.6$ m^2 s^{-1}, which is consistent with Fujita's[18–21] and our previous measurements[22] on the $Pd_{12}L_{24}$ nanosphere (see Supplementary Fig. 17). Cold-spray ionization mass spectroscopy (CSI-MS) also clearly confirmed the presence of $Pd_{12}L_{24}$ spheres with a molecular weight of 17,592 Da, as is evident from the prominent peaks at $[M - x(OTf)]^{x+}$ ($x = 6–11$ (Fig. 1c)). The high resolution of the MS spectra allowed the determination of the elemental composition, which was found to be in line with the simulated spectra of the sphere. The sphere shell already bears 24 positive charges (from Pd^{2+}), which together with the 24 positive charges from the guanidinium groups at the inside of the sphere make a total charge of 48+ (and 48 triflate counter anions). This demonstrates that, despite the high local charge, there is still a strong driving force to form this $M_{12}L_{24}$ assembly.

When a CD_3CN solution of building block **1** (2 equiv.) was stirred in the presence of 1 equiv. $Pt(CH_3CN)_4(OTf)_2$ at 60 °C, the $Pt_{12}L_{24}$ species (**3**) formed overnight, as indicated by the ^{1}H NMR spectra, which show very similar proton chemical shifts to those for the $Pd_{12}L_{24}$ sphere. In line with previous reports, the signals in the ^{1}H NMR spectra are much broader compared with those of the palladium-based spheres because of the restricted tumbling rotation of Pt–pyridine bonds, as suggested by Fujita *et al.*[28]. Again, the DOSY NMR spectra show one clear single band at log

Table 1 | Cyclization of acetylenic acid 4 to give enol lactone 5.

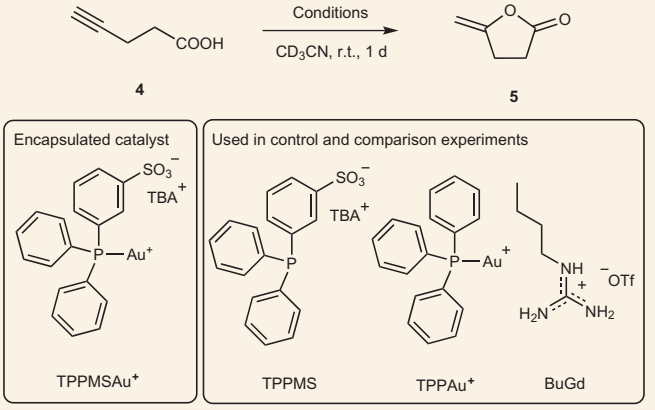

Entry	Conditions	Conversion*	TOF_{ini} (h^{-1})†
1	$TPPMSAu^+$	44%	0.45
2	$TPPMSAu^+$ + sphere	17%	0.14
3	**$TPPMSAu^+$ + sphere + NEt_3**	**>95%**	**5.75**
4	$TPPMSAu^+$ + NEt_3	19%	0.19
5	Sphere	–	–
6	Sphere + NEt_3	2%	n.d.
7	TPPMS + sphere	–	–
8	TPPMS + sphere + NEt_3	–	–
9	$TPPAu^+$	13%	0.11
10	$TPPAu^+$ + sphere	45%	0.33
11	$TPPAu^+$ + sphere + NEt_3	49%	0.66
12	$TPPAu^+$ + NEt_3	17%	0.17
13	$TPPMSAu^+$ + BuGd	25%	0.25
14	$TPPMSAu^+$ + BuGd + NEt_3	36%	0.75

All the reactions were carried out in CD_3CN at room temperature (r.t.) for one day. Reagent concentrations (if applicable): [**4**] = 10 mM, [Au^+] = 0.5 mM, [NEt_3] = 0.5 mM, [sphere **3**] = 3/24 (= 0.125) mM (3 mM building block), [BuGd] = 3 mM, [TPPMS] = 0.5 mM. The cationic Au^+ was generated *in situ* by adding equal equivalents of AgOTf. *The conversion was calculated based on ^{1}H NMR integration by using 1,3,5-trimethoxybenzene as an internal standard (error 5%). †TOF_{ini} was calculated at 15% conversion (error 5%). For full experimental details see the Supplementary Information. n.d., not determined.

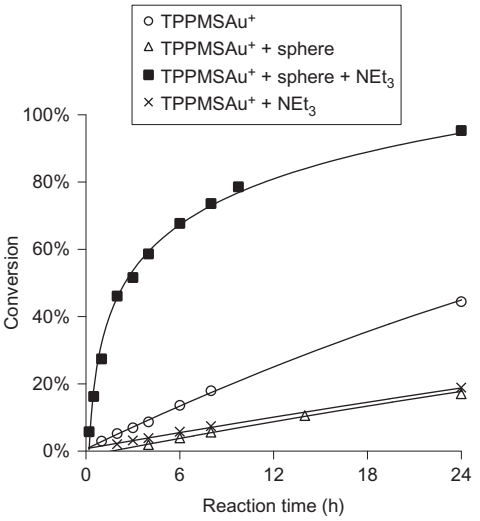

Figure 2 | The reaction progress for the conversion of 4 is displayed for different catalysts. The much higher reaction rates when catalysts and substrates are pre-organized in the sphere are reflected in the steeper conversion curve. For the reaction conditions, see Table 1 (entries 1–4).

$D = -9.6$ m^2 s^{-1}, identical to that observed for the $Pd_{12}L_{24}$ sphere (see Supplementary Fig. 18), which indicates that the Pt and Pd spheres (**3** and **2**) have the same size. Interestingly, the Pt spheres are larger than those reported by Fujita ($Pt_{12}L_{24}$ versus Pt_6L_{12}), probably because other building blocks were used[28].

With the Pd and Pt spheres (**2** and **3**, respectively) that have guanidinium functional groups inside now available, we next evaluated their binding properties with respect to anionic carboxylate and sulfonate guests (as tetra(*n*-butyl)ammonium (TBA^+) salts (see the Supplementary Information)). The 1:1 complex formation of benzoate and *p*-toluenesulfonate with the parent building block **1** was established by NMR titrations, and association constants of 1,850 and 330 M^{-1}, respectively, were found (see the Supplementary Information). A NMR titration of the Pd sphere **2** with benzoate indicated that the sphere disassembled under these conditions. The stable Pt sphere **3** showed partial encapsulation of the benzoate guests, which suggests that the binding in the sphere is of the same magnitude as that for the free building block **1** (~80% encapsulation with 12 equiv. benzoate (see Supplementary Fig. 50)). Both the Pd- and Pt-based spheres are stable in the presence of *p*-toluenesulfonate and fully bind 24 sulfonate guests under the same conditions, as indicated by the DOSY NMR spectra, which show that the guest signals are in line with the sphere band (see Supplementary Figs 38 and 51). Also, in the ^{1}H NMR spectra significant downfield shifts induced by hydrogen bonding were observed for the guanidinium protons H^g and H^h, whereas the other proton signals on the sphere remained approximately the same. The *p*-toluenesulfonate signals also shifted upfield and broadened, which indicates a significant change of the local environment (see Supplementary Figs 37 and 51). When an excess of *p*-toluenesulfonate guests was added, the sphere signals gradually disappeared and precipitation was observed (precipitation was previously reported to be a result of vesicle-like assembly formation[29]). Importantly, at 10 mM concentrations of guanidinium and *p*-toluenesulfonate all the guests are bound, which suggests that the guest is bound much more strongly within the sphere than to the reference ligand **1**. This was further demonstrated in a competitive binding experiment from which the binding to the sphere could be estimated as >10^5 M^{-1}, which is much higher than that observed for the binding to building block **1** (see the Supplementary Information). The strong binding of sulfonate-containing guest molecules in the guanidinium-functionalized sphere is most probably based on multitopic binding, that is, the binding of the sulfonate group by two (or more) adjacent guanidinium-binding sites (see Fig. 1e). Such a binding geometry was previously noted in guanidinium–sulfonate hydrogen-bonding networks, also observed in the solid state[25–27]. Indeed, $Pd_{12}L_{24}$ spheres with 24 quaternary ammonium groups that cannot form such multitopic binding geometry show only weak binding of the monosulfonate guests[30].

This difference in binding strength between the *p*-toluenesulfonate and the benzoate provides interesting opportunities, as we can now functionalize the catalyst with the strong binding unit and the substrate with the weaker binding unit. Along these lines we evaluated the binding of gold complex TPPMSAuCl (TPPMS = triphenylphosphinomonosulfonate), and found that this complex was also fully encapsulated until precipitation was observed, as confirmed by NMR and DOSY (see Supplementary Figs 41–42 and 52) (for some examples of encapsulation of a metal complex within self-assembled M_2L_4 nanocapsules, see Desmarets *et al.*[31,32]). The CSI-MS spectra of sphere **2** mixed with various amounts (6, 12, 18 and 24 equiv.) of TPPMSAuCl clearly showed a series of peaks that corresponded to $[M - x(OTf) + y(TPPMSAuCl)]^{x-y}$. Importantly, the numbers of associated guests (y) correlated with the amounts of the guest added (for 6 equiv., $y = 0$–5; for 12 equiv., $y = 5$–14; for 18 equiv., $y = 13$–21; for 24 equiv., $y = 17$–25) (Supplementary Figs 43–49 and Supplementary Tables 3–6). This shows that the binding of the gold complex TPPMSAuCl is sufficiently strong to identify the supramolecular structures by MS.

Having established that the gold complex TPPMSAuCl is strongly bound at the inside of the spheres and that carboxylate-functionalized

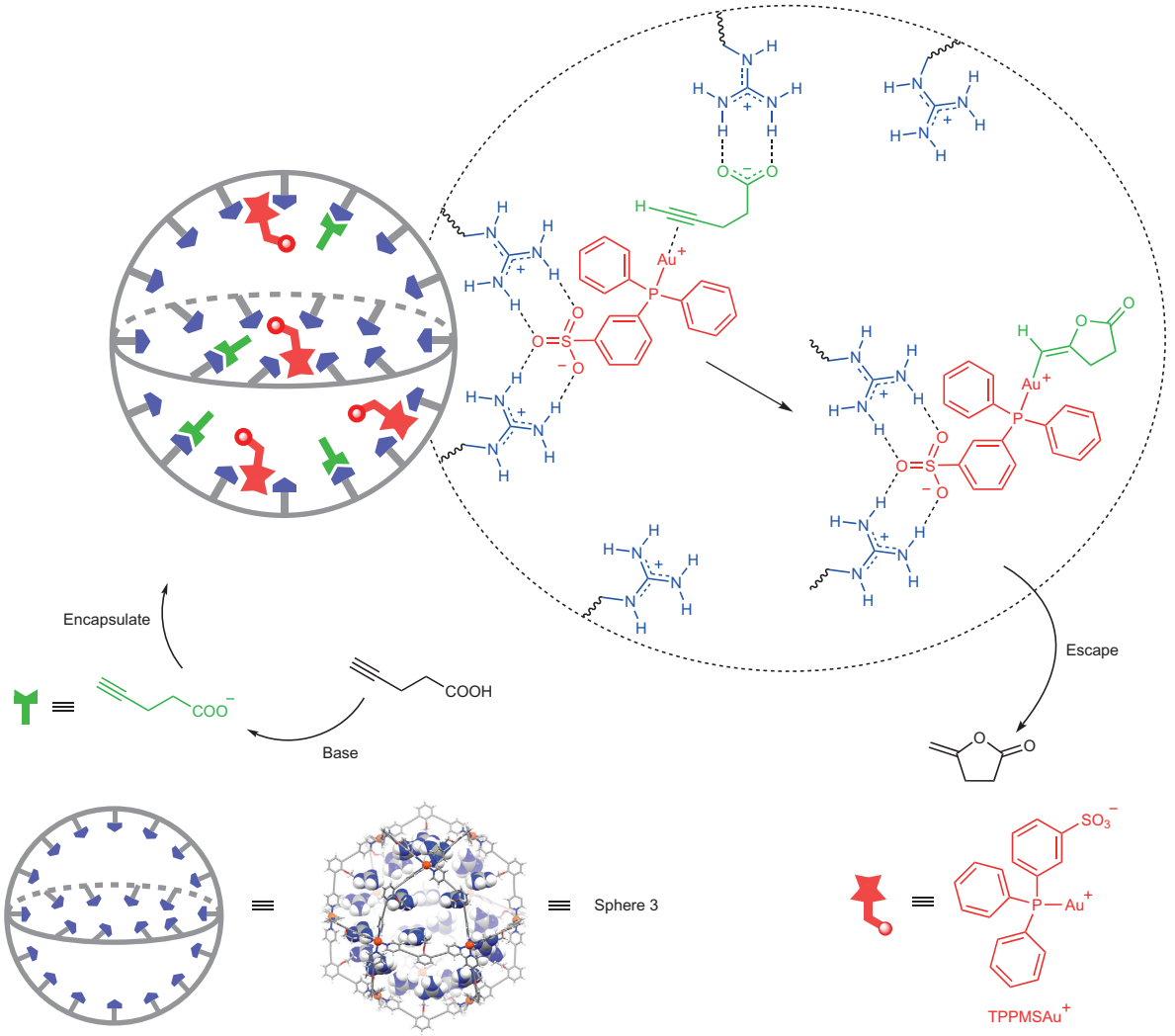

Figure 3 | Schematic representation of the base-triggered catalytic gating process. The gold(I) catalysts (drawn in red) are located in the sphere. Once the substrate (in black) is deprotonated the anionic substrate (in green) enters the sphere to pre-organize close to the catalyst via hydrogen bonding to the guanidine-binding site (displayed in blue). After rapid conversion of the substrate, the neutral cyclic product leaves the sphere.

substrates can be pre-organized in the proximity of the gold complex by weaker binding to the same binding sites, this system was applied in the Au^+-catalysed cyclization reaction of acetylenic acid to give enol lactone[33–35] (Table 1) (for some examples of Au^+-based catalysis through encapsulation by a cage or capsule, see Cavarzan *et al.*[36], Wang *et al.*[37], Hart-Cooper *et al.*[38] and Wang *et al.*[39]). Pt sphere **3** was used for this purpose because of its higher stability compared with that of the Pd sphere, and in none of the catalysis experiments was degradation of the sphere observed. Cationic Au^+ catalysts were generated *in situ* by adding AgOTf to a solution of TPPMSAuCl, and the resulting species were also encapsulated within the sphere, as indicated by DOSY (see Supplementary Fig. 53). In a typical reaction using the sphere as template, 4 equiv. of Au^+ per sphere were present to leave sufficient guanidinium sites for substrate pre-organization in the remaining 20 binding sites. The conversion and the turnover frequency (TOF) (measured at 15% conversion) of all reactions, including the control experiments, are displayed in Table 1 and the reaction profiles of the key experiments are displayed in Fig. 2. The selectivity is not listed in Table 1 as in all reactions only the 5-*exo* product **5** was formed.

Catalytic reactions were performed under several conditions, in the presence or absence of the sphere and in the presence or absence of catalytic amounts of the base. The free catalyst showed a moderate catalytic activity for this reaction (44% conversion, $TOF_{ini} = 0.45\ h^{-1}$ (Table 1, entry 1)). When the same catalyst was inside sphere **3**, however, the reaction was three times slower (Table 1, entry 2). Also, if the reaction was carried out in the presence of catalytic amounts of base (NEt_3) it was three times slower (Table 1, entry 4). In contrast, when a catalytic amount of base (NEt_3) was present and the catalyst was in the sphere, a dramatic increase of the activity was observed (>95% conversion, $TOF_{ini} = 5.75$ (Table 1, entry 3)). Under these conditions, the catalyst is inside the sphere and deprotonated substrates are bound to the free guanidine sites. In the absence of base, the substrates are in acidic form, and as such have no affinity for guanidine. Indeed, separate ^1H NMR and DOSY experiments showed that neutral guests were not bound in the sphere (see Supplementary Fig. 55). The base-triggered (NEt_3) encapsulation of substrate **4** within the sphere was further demonstrated by ^1H NMR and DOSY (see Supplementary Fig. 56).

A series of control experiments was performed to confirm further the template effect of the sphere on this reaction. In the absence of the Au^+ catalysts but in the presence of the sphere no conversion was observed, even in the presence of base and/or the TPPMS ligand (Table 1, entries 5–8). This confirms that, as expected, the catalytic active species is the Au catalyst. Control experiments in which $TPPAu^+$, a complex that is not bound in the sphere (as demonstrated

Table 2 | Effect of competitive *p*-toluenesulfonate binder on cyclization.

Entry	Conditions	Conversion*	TOF_{ini} (h^{-1})†
1	$TPPMSAu^+$ + sphere + NEt_3	>95%	5.75
2	$TPPMSAu^+$ + sphere + NEt_3 + $TolSO_3^-$ (5 equiv.)†	52%	2.42
3	$TPPMSAu^+$ + sphere + NEt_3 + $TolSO_3^-$ (10 equiv.)†	33%	0.49
4	$TPPMSAu^+$ + sphere + NEt_3 + $TolSO_3^-$ (15 equiv.)†	23%	0.20
5	$TPPMSAu^+$ + sphere + NEt_3 + $TolSO_3^-$ (20 equiv.)†	19%	0.21
6	$TPPMSAu^+$ + sphere + $TolSO_3^-$ (20 equiv.)†	13%	0.13
7	$TPPMSAu^+$ + NEt_3 + $TolSO_3^-$ (20 equiv.)†	22%	0.18

The effect of competitive *p*-toluenesulfonate binder on the cyclization of acetylenic acid **4** to give enol lactone **5**. Standard reaction conditions and procedures as in Table 1 were applied and all the conversions were reported after one day at r.t. Reagent concentrations (if applicable): [**4**] = 10 mM, [$TPPMSAu^+$] = 0.5 mM (4 equiv. per sphere), [NEt_3] = 0.5 mM, [sphere **3**] = 0.125 mM. *The error (s.d.) in the determination of the conversion and TOF_{ini} is estimated to be 5% (s.d.). †[$TolSO_3^-$] (as TBA^+ salt) = 0.625, 1.25, 1.88, 2.5, 2.5 and 2.5 mM for entries 2–7, respectively; the number in brackets indicates the equivalents of $TolSO_3^-$ per sphere.

Table 3 | Substrate-selective catalysis using the sphere system.

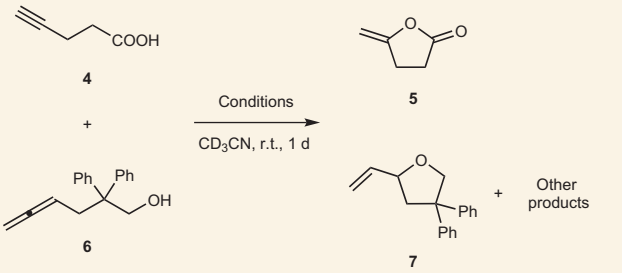

Entry	Conditions	Conversion*	
		4	**6**
1	$TPPMSAu^+$	57%	50%†
2	$TPPMSAu^+$ + sphere	20%	Trace
3	$TPPMSAu^+$ + sphere + NEt_3	81%	–
4	$TPPMSAu^+$ + NEt_3	17%	–

Standard reaction conditions and procedures as in Table 1 were applied, except that an equal molar mixture of **4** (10 mM) and **6** (10 mM) was used. Other reagent concentrations (if applicable): [$TPPMSAu^+$] = 0.5 mM, [NEt_3] = 0.5 mM, [sphere **3**] = 0.125 mM. *All conversions were measured after one day for a clear comparison (error 5%), although the reactions still proceeded. †**7** and other unidentified products were formed.

by DOSY (see Supplementary Fig. 54)), was used as the catalyst gave a conversion that was only slightly affected by the presence of the sphere or base (entries 9–12). Furthermore, the monomeric $TPPMSAu^+$ catalyst was applied in combination with a single guanidinium-binding site, BuGd, which also only affects the reaction to a small extent (entries 13 and 14).

To understand further the effect of substrate pre-organization, additional experiments were designed. The mechanism of a related gold-catalysed cyclization has been studied previously and it was demonstrated that it consists of reversible substrate activation followed by a rate-determining protodeauration[40]. The rate acceleration could therefore be a result of substrate pre-organization (to shift the pre-equilibrium) or the high local concentration of the acidic guanidinium sites that may promote protodeauration[41]. The first experiment that indicated the direction of the substrate pre-organization effect is a classic competition experiment in which strongly binding guests are added that compete for the binding site with the substrate. For this purpose we used the strongly binding *p*-toluenesulfonate guest (*p*-$TolSO_3TBA$, *vide supra*). As is clear from the results displayed in Table 2, the rate decreases with increasing concentration of *p*-toluenesulfonate (Table 2, entries 1–5). When the guanidinium sites are all occupied by the sulfonate-containing catalysts and *p*-toluenesulfonate guests (Table 2, entry 5), there is no remaining cage-acceleration effect (Table 2, entry 5 versus entry 7). As the proton concentration is the same, this result clearly supports the substrate pre-organization effect.

In a second, complementary experiment, we studied the gold-catalysed cyclization of *N*-acyl propargylamines, for which a similar protodeauration as the rate-determining step[42] was reported. These substrates, however, do not have a carboxylate function that leads to pre-organization via the binding sites in the sphere, and if rate acceleration is observed for these substrates this would be caused by local proton-concentration effects. From a series of experiments with the *N*-acetyl and *N*-benzoyl propargylamine substrates, it is clear that the presence of the sphere has a negligible effect on the cyclization reaction (see Supplementary Table 8). This demonstrates that the acidic guanidinium sites around the catalyst do not accelerate the protodeauration step for these reactions, which again implies that the acceleration we observed for the alkyne acid substrate can be ascribed to the pre-organization of the substrate by binding to the guanidinium sites in the sphere.

These experiments together show that we can bind our sulfonate-containing catalyst in the sphere, and pre-organize the carboxylate-functionalized substrates nearby, which overall leads to a tenfold increase in the reaction rate. In the absence of base, there is no driving force for the neutral substrate molecules to enter the sphere, and as such the catalysts are rather shielded, which leads to low reaction rates. By adding catalytic amounts of base (4 equiv. per sphere), the deprotonated substrates enter the sphere to bind to the guanidinium sites. The product that forms is neutral, and as such has no affinity for the binding site, which prevents product-inhibition effects by competitive binding in the sphere. As there is no thermodynamic driving force for neutral guests to enter, the current supramolecular system provides a tool to control the access of the substrate to the catalyst sites, which implies gating (Fig. 3). An assembly system that brings 24 guanidinium sites together allows multiple guanidinium sites to participate cooperatively in the pre-organization of the substrate and catalyst; for example, two (or more) adjacent guanidinium sites hold one sulfonate catalyst and another neighbour guanidinium site pre-organizes the carboxylate substrate around it (Fig. 3).

The difference in affinity for anionic and neutral guests provides the opportunity to use these systems for substrate-selective catalysis[43]. To demonstrate this principle, we used the sphere-enclosed gold catalyst to convert, in a competition experiment, an equal molar mixture of acetylenic acid substrate **4** and allenol substrate **6** (Table 3). Under these conditions only substrate **4** was converted with a high conversion (81%, Table 3, entry 3), whereas in the absence of the sphere both substrates were converted to a similar extent (Table 3, entry 1). Combining the active catalyst with solely the sphere or base resulted in only a low conversion of substrate **4** (Table 3, entries 2 and 4).

Conclusions

In conclusion, $M_{12}L_{24}$ spheres functionalized with 24-fold endohedral guanidinium-binding motifs were prepared. The multiple guanidinium sites in a confined space resulted in a strong binding of sulfonate guests ($>10^5\ M^{-1}$) as the high local concentration facilitates cooperative binding. Carboxylate guests still bind in a 1:1 ratio and, as such, the binding is much weaker (by $10^3\ M^{-1}$). This difference makes these nanospheres perfect vehicles for substrate/catalyst pre-organization: four sulfonate-containing $TPPMSAu^+$ catalysts were strongly bound within the sphere and acetylenic carboxylate substrates were pre-organized by adjacent guanidinium sites for an efficient cyclization to give the enol lactone. The neutral analogue of the substrate, acetylenic acid, has no driving force to

enter, and as such is slowly converted by the sphere-encapsulated catalysts. Base-triggered co-encapsulation of the substrates within the sphere increases the rate 40-fold. As many catalyst complexes are utilized with sulfonate groups, generally to make them water soluble, we believe that this may be a general strategy that is applicable to many different reactions. As well as the pre-organization effect, the base-controlled access of substrates to the catalysts, facilitated by the protecting sphere, is a finding that could be useful in the development of more-complex catalyst systems.

Received 21 August 2015; accepted 18 November 2015; published online 11 January 2016

References

1. van Leeuwen, P. W. N. M. *Supramolecular Catalysis* (Wiley-VCH, 2008).
2. Raynal, M., Ballester, P., Vidal-Ferran, A. & van Leeuwen, P. W. N. M. Supramolecular catalysis. Part 1: non-covalent interactions as a tool for building and modifying homogeneous catalysts. *Chem. Soc. Rev.* **43,** 1660–1733 (2014).
3. Raynal, M., Ballester, P., Vidal-Ferran, A. & van Leeuwen, P. W. N. M. Supramolecular catalysis. Part 2: artificial enzyme mimics. *Chem. Soc. Rev.* **43,** 1734–1787 (2014).
4. Meeuwissen, J. & Reek, J. N. H. Supramolecular catalysis beyond enzyme mimics. *Nature Chem.* **2,** 615–621 (2010).
5. Breit, B. Supramolecular approaches to generate libraries of chelating bidentate ligands for homogeneous catalysis. *Angew. Chem. Int. Ed.* **44,** 6816–6825 (2005).
6. Dydio, P. & Reek, J. N. H. Supramolecular control of selectivity in transition-metal catalysis through substrate preorganization. *Chem. Sci.* **5,** 2135–2145 (2014).
7. Breslow, R. & Dong, S. D. Biomimetic reactions catalyzed by cyclodextrins and their derivatives. *Chem. Rev.* **98,** 1997–2011 (1998).
8. Hooley, R. J. & Rebek, J. Jr. Chemistry and catalysis in functional cavitands. *Chem. Biol.* 255–264 (2009).
9. Dong, Z., Luo, Q. & Liu, J. Artificial enzymes based on supramolecular scaffolds. *Chem. Soc. Rev.* **41,** 7890–7908 (2012).
10. Vriezema, D. M. *et al.* Self-assembled nanoreactors. *Chem. Rev.* **105,** 1445–1489 (2005).
11. Fiedler, D., Leung, D. H., Bergman, R. G. & Raymond, K. N. Selective molecular recognition, C–H bond activation, and catalysis in nanoscale reaction vessels. *Acc. Chem. Res.* **38,** 351–360 (2005).
12. Koblenz, T. S., Wassenaar, J. & Reek, J. N. H. Reactivity within a confined self-assembled nanospace. *Chem. Soc. Rev.* **37,** 247–262 (2008).
13. Pluth, M. D., Bergman, R. G. & Raymond, K. N. Proton-mediated chemistry and catalysis in a self-assembled supramolecular host. *Acc. Chem. Res.* **42,** 1650–1659 (2009).
14. Yoshizawa, M., Klosterman, J. K. & Fujita, M. Functional molecular flasks: new properties and reactions within discrete, self-assembled hosts. *Angew. Chem. Int. Ed.* **48,** 3418–3438 (2009).
15. Wiester, M. J., Ulmann, P. A. & Mirkin, C. A. Enzyme mimics based upon supramolecular coordination chemistry. *Angew. Chem. Int. Ed.* **50,** 114–137 (2011).
16. Amouri, H., Desmarets, C. & Moussa, J. Confined nanospaces in metallocages: guest molecules, weakly encapsulated anions, and catalyst sequestration. *Chem. Rev.* **112,** 2015–2041 (2012).
17. Leenders, S. H. A. M., Gramage-Doria, R., de Bruin, B. & Reek, J. N. H. Transition metal catalysis in confined spaces. *Chem. Soc. Rev.* **44,** 433–448 (2015).
18. Tominaga, M., Suzuki, K., Murase, T. & Fujita, M. 24-Fold endohedral functionalization of a self-assembled $M_{12}L_{24}$ coordination nanoball. *J. Am. Chem. Soc.* **127,** 11950–11951 (2005).
19. Harris, K., Fujita, D. & Fujita, M. Giant hollow M_nL_{2n} spherical complexes: structure, functionalisation and applications. *Chem. Commun.* **49,** 6703–6712 (2013).
20. Harris, K., Sun, Q.-F., Sato, S. & Fujita, M. $M_{12}L_{24}$ spheres with *endo* and *exo* coordination sites: scaffolds for non-covalent functionalization. *J. Am. Chem. Soc.* **135,** 12497–12499 (2013).
21. Bruns, C. J. *et al.* Emergent ion-gated binding of cationic host–guest complexes within cationic $M_{12}L_{24}$ molecular flasks. *J. Am. Chem. Soc.* **136,** 12027–12034 (2014).
22. Gramage-Doria, R. *et al.* Gold(I) catalysis at extreme concentrations inside self-assembled nanospheres. *Angew. Chem. Int. Ed.* **53,** 13380–13384 (2014).
23. Best, M. D., Tobey, S. L. & Anslyn, E. V. Abiotic guanidinium containing receptors for anionic species. *Coord. Chem. Rev.* **240,** 3–15 (2003).
24. Schug, K. A. & Lindner, W. Noncovalent binding between guanidinium and anionic groups: focus on biological- and synthetic-based arginine/guanidinium interactions with phosph[on]ate and sulf[on]ate residues. *Chem. Rev.* **105,** 67–113 (2005).
25. Burrows, A. D., Harrington, R. W., Mahon, M. F. & Teat, S. J. Structural manipulation of hydrogen bond networks using sulfonated phosphane ligands and their complexes: competition and interplay between strong and weak hydrogen bonds. *Eur. J. Inorg. Chem.* 1433–1439 (2003).
26. Russell, V. A., Etter, M. C. & Ward, M. D. Layered materials by molecular design: structural enforcement by hydrogen bonding in guanidinium alkane- and arenesulfonates. *J. Am. Chem. Soc.* **116,** 1941–1952 (1994).
27. Xiao, W., Hu, C. & Ward, M. D. Guest exchange through single crystal–single crystal transformations in a flexible hydrogen-bonded framework. *J. Am. Chem. Soc.* **136,** 14200–14206 (2014).
28. Fujita, D., Takahashi, A., Sato, S. & Fujita, M. Self-assembly of Pt(II) spherical complexes via temporary labilization of the metal–ligand association in 2,2,2-trifluoroethanol. *J. Am. Chem. Soc.* **133,** 13317–13319 (2011).
29. Li, D. *et al.* Viral-capsid-type vesicle-like structures assembled from $M_{12}L_{24}$ metal–organic hybrid nanocages. *Angew. Chem. Int. Ed.* **50,** 5182–5187 (2011).
30. Kikuchi, T., Murase, T., Sato, S. & Fujita, M. Polymerisation of an anionic monomer in a self-assembled $M_{12}L_{24}$ coordination sphere with cationic interior. *Supramol. Chem.* **20,** 81–94 (2008).
31. Desmarets, C., Ducarre, T., Rager, M. N., Gontard, G. & Amouri, H. Self-assembled M_2L_4 nanocapsules: synthesis, structure and host–guest recognition toward square planar metal complexes. *Materials* **7,** 287–301 (2014)
32. Desmarets, C., Gontard, G., Cooksy, A. L., Rager, M. N. & Amouri, H. Encapsulation of a metal complex within a self-assembled nanocage: synergy effects, molecular structures, and density functional theory calculations. *Inorg. Chem.* **53,** 4287–4294 (2014).
33. Genin, E. *et al.* Room temperature Au(I)-catalyzed *exo*-selective cycloisomerization of acetylenic acids: an entry to functionalized γ-lactones. *J. Am. Chem. Soc.* **128,** 3112–3113 (2006).
34. Harkat, H., Weibel, J.-M. & Pale, P. A mild access to γ- or δ-alkylidene lactones through gold catalysis. *Tetrahedron Lett.* **47,** 6273–6276 (2006).
35. Lee, L.-C. & Zhao, Y. Metalloenzyme-mimicking supramolecular catalyst for highly active and selective intramolecular alkyne carboxylation. *J. Am. Chem. Soc.* **136,** 5579–5582 (2014).
36. Cavarzan, A., Scarso, A., Sgarbossa, P., Strukul, G. & Reek, J. N. H. Supramolecular control on chemo- and regioselectivity via encapsulation of (NHC)-Au catalyst within a hexameric self-assembled host. *J. Am. Chem. Soc.* **133,** 2848–2851 (2011).
37. Wang, Z. J., Brown, C. J., Bergman, R. G., Raymond, K. N. & Toste, F. D. Hydroalkoxylation catalyzed by a gold(I) complex encapsulated in a supramolecular host. *J. Am. Chem. Soc.* **133,** 7358–7360 (2011).
38. Hart-Cooper, W. M., Clary, K. N., Toste, F. D., Bergman, R. G. & Raymond, K. N. Selective monoterpene-like cyclization reactions achieved by water exclusion from reactive intermediates in a supramolecular catalyst. *J. Am. Chem. Soc.* **134,** 17873–17876 (2012).
39. Wang, Z. J., Clary, K. N., Bergman, R. G., Raymond, K. N. & Toste, F. D. A supramolecular approach to combining enzymatic and transition metal catalysis. *Nature Chem.* **5,** 100–103 (2013).
40. Brown, T. J., Weber, D., Gagné, M. R. & Widenhoefer, R. A. Mechanistic analysis of gold(I)-catalyzed intramolecular allene hydroalkoxylation reveals an off-cycle bis(gold) vinyl species and reversible C–O bond formation. *J. Am. Chem. Soc.* **134,** 9134–9137 (2012).
41. Shu, X.-Z. *et al.* Silica-supported cationic gold(I) complexes as heterogeneous catalysts for regio- and enantioselective lactonization reactions. *J. Am. Chem. Soc.* **137,** 7083–7086 (2015).
42. Wang, W., Hammond, G. B. & Xu, B. Ligand effects and ligand design in homogeneous gold(I) catalysis. *J. Am. Chem. Soc.* **134,** 5697–5705 (2012).
43. Lindbäck, E., Dawaigher, S. & Wärnmark, K. Substrate-selective catalysis. *Chem. Eur. J.* **20,** 13432–13481 (2014).

Acknowledgements

Financial support was provided by the University of Amsterdam and by the European Research Council (Advanced Grant C.2322.0269). P. Li and W. I. Dzik are acknowledged for X-ray crystallography studies. B. de Bruin, J. I. van der Vlugt, W. I. Dzik and R. Gramage-Doria are also acknowledged for helpful discussions.

Author contributions

J.N.H.R. and Q.Q.W. conceived and designed the experiments. Q.Q.W. and S.G. performed the experiments and analysed the data. M.D. and I.I.-B. carried out the CSI-MS measurements and analysed the data. J.N.H.R. and Q.Q.W. wrote the manuscript. J.N.H.R., Q.Q.W., S.G. and S.H.A.M.L. discussed the results and edited the manuscript.

Additional information

Supplementary information is available in the online version of the paper. Reprints and permissions information is available online at www.nature.com/reprints. Correspondence and requests for materials should be addressed to J.N.H.R.

Competing financial interests

The authors declare no competing financial interests.